



## On the energy measurement of jets in high-energy physics experiments

Sehwook Lee, Richard Wigmans\*

Texas Tech University, Lubbock, TX, USA

### ARTICLE INFO

#### Article history:

Received 3 October 2012

Received in revised form

10 December 2012

Accepted 28 January 2013

Available online 6 February 2013

#### Keywords:

Calorimetry

Jets

Non-compensation effects

Jet energy corrections

### ABSTRACT

As the energies at which the elementary structure of matter is studied increased, the emphasis in scattering experiments has shifted from detecting individual hadrons to fragmenting quarks and gluons, which manifest themselves as particle jets. In this paper, we investigate and quantify some systematic effects that affect the precision with which the properties of the fragmenting constituents can be determined. We concentrate on the calorimeters that are used to measure the energies, and in particular on how the non-compensating nature of a calorimeter affects the energy measurement of different types of partons.

© 2013 Elsevier B.V. All rights reserved.

### 1. Introduction

In the past 50 years, the center-of-mass energy of particle-particle collisions at accelerators has increased by three orders of magnitude, from  $\sim 8$  GeV at CERN's Proton Synchrotron [1] and Brookhaven's Alternating Gradient Synchrotron [2] to 8 TeV at CERN's Large Hadron Collider [3]. Whereas experiments at the PS and AGS emphasized reconstructing the 4-vector of each particle produced in the interactions, modern collider experiments select events primarily on the basis of *energy flow variables*, such as total transverse energy, missing (transverse) energy as well as the occurrence of *jets*. Jets were first observed in the 1970s, in particular at  $e^+e^-$  colliders such as SPEAR [4] and PETRA [5]. The non-isotropic distribution of the reaction products, characterized by variables such as *sphericity* and *spherocity* led to the notion that one was observing the end products of the fragmentation of quarks, antiquarks and gluons produced in the collisions.

As the accelerator energy increased, the emphasis in scattering experiments shifted more and more to detecting particle jets as the primary carriers of information about the collisions in which they were produced. Because of kinematics, jets became also much more collimated, and thus recognizable as such in this process. Whereas in the early days uncertainty in the experimental properties of the underlying constituent were dominated by questions as to which final-state particles to include and exclude as products of the fragmentation process, in modern

experiments the properties of the particle detectors are more and more becoming the limiting factor in this respect.

All experiments at modern particle accelerators use calorimeters to detect jets and measure their properties. The calorimeters suffer from a very inconvenient problem, namely the fact that their response, *i.e.*, the average signal produced per unit of energy deposited by the absorbed particle, is different for hadronic and non-hadronic energy deposits. This is commonly referred to as non-compensation [6], and the extent of this problem is quantified with the so-called  $e/h$  ratio.

In some experiments, one tries to improve the quality of jet measurements by using the tracking system to measure the momenta of the charged jet fragments. This can of course be done with great precision but creates a major problem since one has to eliminate the contribution of these fragments to the calorimeter signals in order to avoid double counting. It has been demonstrated that this method, known as Particle Flow Analysis (PFA), especially benefits experiments in which the calorimetric jet measurements leave much to be desired, while experiments with a good calorimeter system do not gain (much) in performance [7]. In practice, this method has been found to improve the jet energy resolution of some LEP experiments [8], as well as the hadron collider experiments CDF (Tevatron) [9] and CMS (LHC) [10]. On the other hand, D0 (Tevatron) and ATLAS (LHC) have not seen any improvement in energy resolution as a result of using PFA algorithms.

It should be emphasized that, even *if* PFA methods would succeed in *completely* eliminating the contribution of the charged jet fragments from the calorimeter signals, one would still need the hadronic calorimeter to measure the energy of neutral jet fragments such as  $K_L^0$  and neutrons. These measurements would also be strongly affected by non-compensation effects.

\* Corresponding author. Tel.: +1 806 742 3779; fax: +1 806 742 1182.  
E-mail address: [wigmans@ttu.edu](mailto:wigmans@ttu.edu) (R. Wigmans).

In this paper, we study the effects of the non-compensation problems on the measurement of the energy of different types of (anti)quarks. We use  $Z^0$  bosons produced in different colliders as the source of the jets. In this way, we can easily distinguish between the different fragmenting partons, since hadronically decaying  $Z^0$ s either produce  $u\bar{u}$ ,  $d\bar{d}$ ,  $s\bar{s}$ ,  $c\bar{c}$  or  $b\bar{b}$  parton pairs in the final state. All events are generated with PYTHIA 8.162 [11]. The energy dependence of the effects is studied by considering  $Z^0$  production at the LHC [3], the Tevatron [12] and LEP I [13]. In Section 2, we review the relevant calorimeter properties. The results of the simulations are described in Section 3. The response to different types of jets in representative calorimeter systems and at different energies is the topic of Section 4, and conclusions are given in Section 5.

## 2. Relevant calorimeter properties

In a calorimeter, high-energy particles are absorbed in a process called shower development.<sup>1</sup> The calorimeter generates signals that are indicative for the energy deposited by the showering particles. If these particles are electrons or photons, their entire energy is typically deposited through electromagnetic processes, and the resulting calorimeter signal is directly proportional to the energy of the incoming particle. Hadron showers consist of two distinctly different components:

1. An *electromagnetic* (em) component:  $\pi^0$ s and  $\eta$ s generated in the absorption process decay into  $\gamma$ s which develop em showers.
2. A *non-electromagnetic* component, which combines essentially everything else that takes place in the absorption process.

For the purpose of calorimetry, the main difference between these components is that some fraction of the energy contained in the non-em component does *not* contribute to the signals. The numerous nuclear reactions that take place in the absorption process are responsible for the overwhelming majority of this *invisible energy*. The nuclear binding energy of the released protons, neutrons and heavier aggregates has to be supplied by the shower particles that induce the reactions and does not contribute to the signals. Other contributions to the invisible energy come from neutrinos and muons that escape the calorimeter.

The invisible energy may represent a considerable fraction of the total energy deposited in the calorimeter. If we define the *response* as the average calorimeter signal per unit of energy, and the responses to the em and non-em shower components as  $e$  and  $h$ , respectively, then the  $e/h$  ratio quantifies the importance of invisible energy effects for a given calorimeter. For example, in some crystal calorimeters  $e/h > 2$ , which means that, on average, more than half of the non-em energy is invisible.

Let  $f_{em}$  be the fraction of the total shower energy contained in the em shower component. Among the characteristics of this component that have profound implications for the performance of hadron calorimeters, we mention:

- (1) The fact that  $\langle f_{em} \rangle$  increases with energy. This effect, which is illustrated in Fig. 1a, is directly responsible for the *intrinsic hadronic signal non-linearity* exhibited by all non-compensating hadronic calorimeters (*i.e.*, calorimeters with  $e/h \neq 1$ ).

<sup>1</sup> In the literature, the term *showering* is also sometimes used for some aspects of the process in which partons are transformed into particle jets. In this paper, we use this term exclusively for processes taking place in the absorption of the jet fragments in a calorimeter. The process in which partons convert into particle jets will be referred to as “fragmentation”.

The figure shows that the em shower component typically represents about half of the total energy, and that  $\langle f_{em} \rangle$  not only depends on the energy, but also on the type of absorber material.

- (2) Event-to-event fluctuations in  $f_{em}$  are large and non-Gaussian. They tend to dominate the energy resolution of non-compensating hadron calorimeters. Fig. 1b shows a measurement of these fluctuations for showers initiated by 150 GeV  $\pi^-$  in a lead-based hadron calorimeter. The observed asymmetry in this distribution is the cause of the *asymmetric response function* (line shape) observed for pions in non-compensating calorimeters. See Fig. 2a for an example. In showers induced by pions, the probability of an anomalously large  $f_{em}$  value is not equal to that of a similarly anomalous small value. The reason for that is the *leading-particle effect*. A large  $f_{em}$  value occurs when in the first nuclear interaction a large fraction of the energy carried by the incoming pion is transferred to a  $\pi^0$ . However, when a similarly large fraction is transferred to another type of particle, the result is not necessarily a small  $f_{em}$  value, since this other particle may produce energetic  $\pi^0$ s in subsequent reactions. Hence the asymmetric response function.
- (3) However, the fluctuations in  $f_{em}$  are not necessarily asymmetric, for example, in showers induced by high-energy protons or kaons.
- (4) In proton-induced showers, the leading particle always has to be a baryon, and the  $\pi^0$ s that determine the  $f_{em}$  value are only produced in later stages of the fragmentation process. As a result, asymmetries such as the ones discussed above are absent, as can be seen in Fig. 2b. Also, since the leading particle typically carries a large fraction of the energy of the incoming particle, the average value of  $f_{em}$ , and thus the response of a calorimeter with  $e/h > 1$ , is smaller for protons than for pions of the same energy. The latter effect is also illustrated in Fig. 2, where the response to 300 GeV protons was measured to be 15% smaller than to 300 GeV pions.
- (5) Similar effects should also be expected for the calorimetric detection of kaons. Since strangeness is conserved in the strong interaction, the leading particle cannot be a  $\pi^0$  either in this case. Therefore, the calorimeter response and the line shape should be affected in a similar way as for protons.

If we normalize the calorimeter response to electrons, then the hadronic response to particles of a given energy can be calculated as follows:

$$R = \langle f_{em} \rangle + [1 - \langle f_{em} \rangle] \frac{h}{e} \quad (1)$$

where  $\langle f_{em} \rangle$  is a function of the energy, but also of the type of hadron. In particular, it is smaller for baryons and kaons than for pions. In this study, we have used Groom’s parameterization of the em shower fraction [16]:

$$\langle f_{em}(E) \rangle = 1 - \left[ \frac{E}{E_0} \right]^{(k-1)}. \quad (2)$$

The parameter  $E_0$ , which describes the average energy needed for the production of a pion in the shower development, has been given a value of 0.7 GeV throughout this analysis. This value gives typically a good description of calorimeters consisting of iron or copper as absorber material (see also Fig. 1a). For the parameter  $k$ , which is a measure for the average multiplicity in the nuclear reactions, we have chosen the value 0.82, which is known to give a good description of a variety of experimental data [6].

One of the most extensive, systematic experimental calorimeter response studies ever has been carried out by the CMS collaboration [18]. Their calorimeter system consists of an em section made of

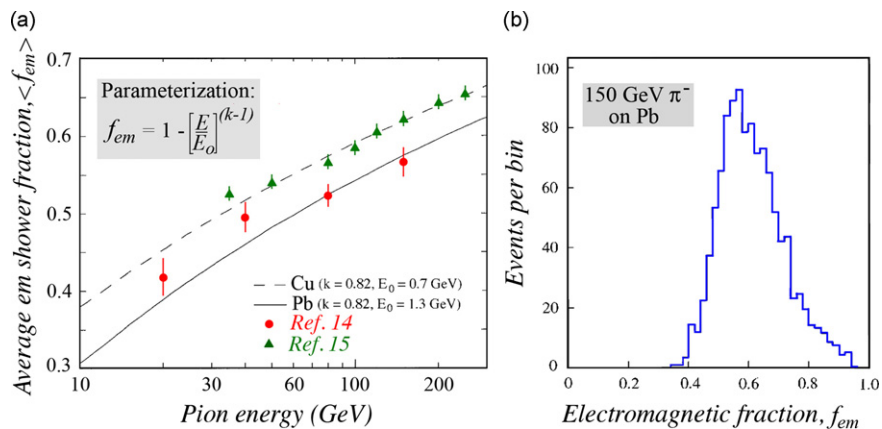


Fig. 1. The average em fraction of showers initiated by pions in lead and copper-based calorimeters, measured as a function of the pion energy (a). Event-to-event fluctuations in the em shower fraction (b). Experimental data from Refs. [14,15] and parameterization from Ref. [16].

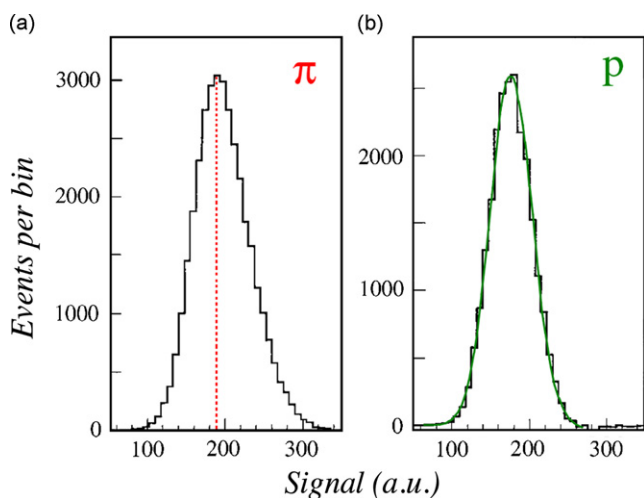


Fig. 2. Signal distributions for 300 GeV pions and protons detected with the CMS HF quartz-fiber calorimeter. The dotted line in (a) corresponds to the most probable signal value (illustrating the asymmetric nature of the pion signal distribution), the curve in (b) represents the result of a Gaussian fit to the proton distribution [17].

PbWO<sub>4</sub> crystals, followed by a hadronic section consisting of brass absorber interleaved with active layers consisting of plastic scintillating material. Both sections were calibrated with electrons, and the response to these particles was set to 1.0 in the following. Fig. 3 shows a compilation of their results for pions, kaons, protons and antiprotons. These results cover an energy range from 2 to 300 GeV. They confirm that the hadronic response is indeed strongly dependent on the energy of the incoming particles. They also confirm that the response to kaons and protons is systematically lower than the response to pions, as explained above. The pion data are well described by Eqs. (1) and (2), using an effective  $e/h$  value of 2.0 for this calorimeter system. This relatively large  $e/h$  value is a consequence of the use of crystals, where on average about half of the available energy is deposited.

In the following, we have simulated the jet response for calorimeter systems with  $e/h$  values of 2.0 (as in CMS), 1.6 (a value representative for calorimeter systems such as the one used in the ATLAS experiment at the LHC), and 1.0. The latter value, which represents a compensating calorimeter system, was chosen as a reference. By comparing its response with that of the other systems, the effects of non-compensation could be assessed.

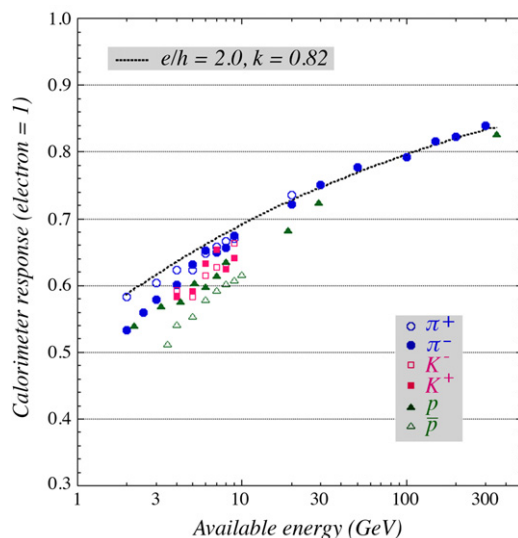


Fig. 3. The response of the CMS calorimeter system to different particles, as a function of energy [18]. Both sections of the calorimeter system were calibrated with electrons, i.e., the response for these particles was set to 1. The dashed curve represents the theoretical hadronic response for a calorimeter with  $e/h=2.0$ , for  $k=0.82$  (see Eqs. (1) and (2)).

### 3. Jet simulations

One of the main goals of this study was to investigate to what extent the energy reconstructed by the calorimeter system depends on the type of parton that fragments into a jet. To this end, we have selected interactions in which hadronically decaying  $Z^0$  bosons were produced. Since our main purpose was to study the parton dependence of the calorimeter effects, we did not attempt to separate the final-state particles from the decay into subsets belonging to the fragmentation of the individual partons produced in the decay. In other words, we considered all final-state particles resulting from the primary process  $Z^0 \rightarrow q\bar{q}$  the end products of two fragmenting quarks and did not attempt to reconstruct separate  $q$  and  $\bar{q}$  jets.

We also did not take into account any possible effects of jet defining algorithms. In practice, one uses such algorithms to select which of the experimentally observed particles produced in the collisions belong to the fragmentation process one wants to study and which do not. Magnetic fields tend to bend soft jet fragments away from the calorimeter area where the more energetic ones end up. They also may “contaminate” the jet by bending

unrelated particles into the conical region around the jet axis. At low collision energies, the uncertainties introduced by such effects tended to dominate the jet energy resolution. However, as the collision energy increased and jets became increasingly collimated, these effects have become less important.

We used PYTHIA 8.162 [11] to simulate the collisions, the decay of the  $Z^0$ s and the fragmentation of the partons produced in this decay. All simulations took Initial State Radiation (ISR), Final State Radiation and Multi-Parton (MP) Interactions fully into account. Each event produced by PYTHIA has an event history, and every step in this history has an index. Using this index, one can trace back each final-state particle to the process in which it was produced. Of course, final-state particles not associated with the decay of a  $Z^0$  produced in a hard-scattering process were excluded in our analyses. This applied, for example, to final-state particles associated with ISR and MP interactions. However, final-state particles associated with the radiation of a gluon by the quark/antiquark pair produced in  $Z^0$  decay were included.

Fig. 4 shows the energy spectra of the  $Z^0$  bosons produced in pp collisions at the Large Hadron Collider at a center-of-mass energy  $\sqrt{s} = 8$  TeV. On average, these  $Z^0$ s carried an energy of 415 GeV. The rms value of the distribution was about as large as the mean value. Especially in order to study the energy dependence of the effects, we

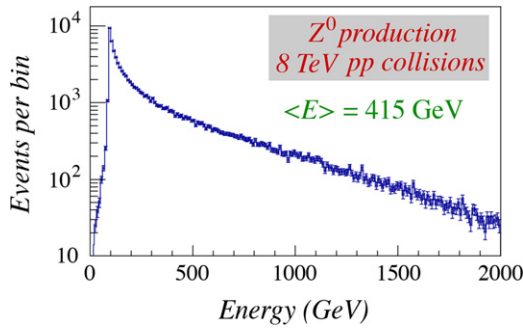


Fig. 4. Energy spectra of the  $Z^0$  bosons produced in 8 TeV pp collisions at the LHC. These particles were used as the source of the different parton jets.

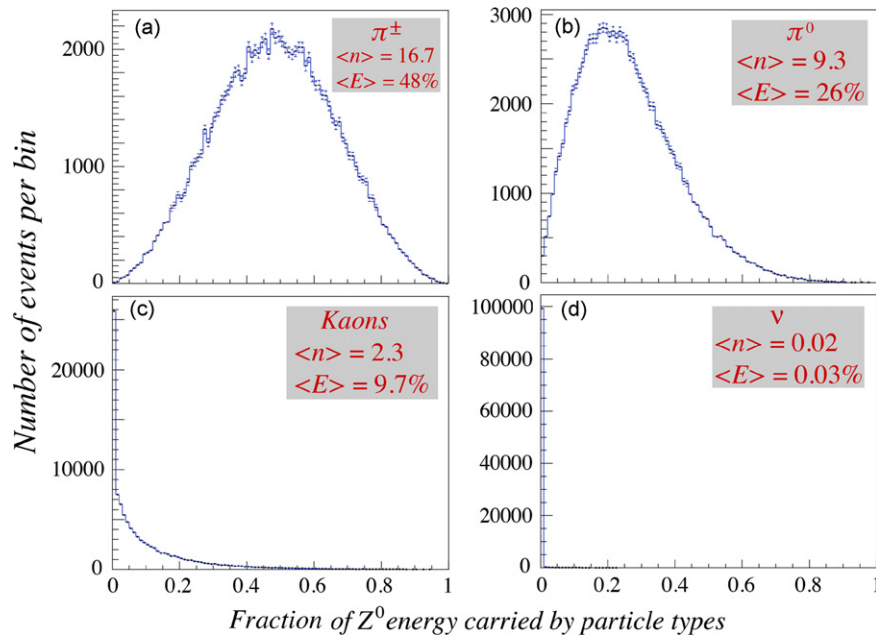


Fig. 5. Distributions of the fractions of the energy of  $Z^0$ s decaying into a  $u\bar{u}$  quark–antiquark pair carried by final-state charged pions (a), neutral pions (b), kaons (c) and (anti)neutrinos (d). The  $Z^0$ s were produced in pp collisions at 8 TeV, as simulated with PYTHIA 8.162.

also used subsets of events in which  $Z^0$ s were produced with energies within a certain bracket. For example, in the 8 TeV pp collisions, we selected a subset of events in which the  $Z^0$  bosons carried a total energy between 0.8 and 1.2 TeV. This bracket represented the highest energy used in our study.

We also used event samples of  $Z^0$  bosons produced in  $p\bar{p}$  collisions at the Tevatron, at  $\sqrt{s} = 1.96$  TeV. And for the production of  $Z^0$  bosons at rest, we simulated  $e^+e^-$  collisions at  $\sqrt{s} = 91$  GeV, as in LEP I.

The  $Z^0$  bosons decayed into  $u\bar{u}$ ,  $d\bar{d}$ ,  $s\bar{s}$ ,  $c\bar{c}$ , or  $b\bar{b}$  quark–antiquark pairs. In each of the mentioned collision scenarios, 100,000 events were simulated for each  $Z^0$  decay mode. For each  $Z^0$  boson generated in these collisions, the complete fragmentation into final-state particles was simulated. As indicated above, the final state also included the end products of gluons radiated in this process. For the analyses described in this paper, the final-state particles were grouped into the following categories: Charged pions,  $\pi^0$ s, kaons, (anti)baryons ( $p, n, \bar{p}, \bar{n}$ ),  $\gamma$ s from sources other than  $\pi^0$  decay (e.g.,  $\eta$  decay),  $e^\pm$ ,  $\mu^\pm$  and (anti)neutrinos. Figs. 5 and 6 show distributions that indicate to what extent some of the mentioned particles appear in the final state of  $Z^0 \rightarrow u\bar{u}$  and  $Z^0 \rightarrow b\bar{b}$  decay, respectively. The most striking differences between these two cases concern the extent to which kaons and (anti)neutrinos are produced in the fragmentation process. The semi-leptonic decay of b quarks and the fact that strange particles are naturally produced in the decay chain of these heavy objects leads to substantially increased branching fractions for kaons and (anti)neutrinos, compared to the  $Z^0 \rightarrow u\bar{u}$  case.

## 4. The calorimeter jet response

### 4.1. Parton dependence

We calculated the jet responses for three different calorimeter systems. One system was modeled after that used in the CMS experiment, of which measured response data for individual hadrons are given in Fig. 3. As shown in Section 2, this calorimeter system was well described with an  $e/h$  value of 2.0. We also used

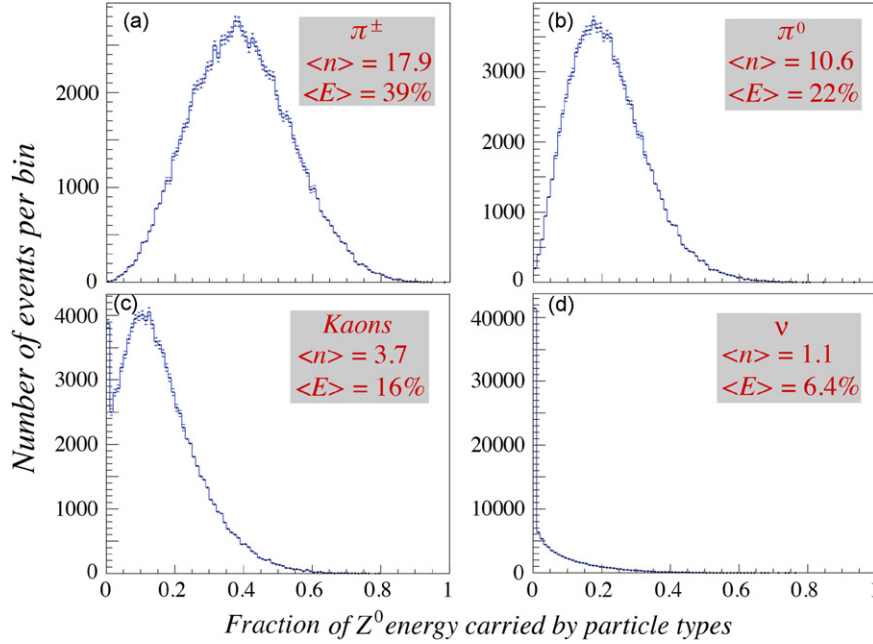


**Fig. 6.** Distributions of the fractions of the energy of  $Z^0$ s decaying into a  $b\bar{b}$  quark-antiquark pair carried by final-state charged pions (a), neutral pions (b), kaons (c) and (anti)neutrinos (d). The  $Z^0$ s were produced in pp collisions at 8 TeV, as simulated with PYTHIA 8.162.

a generic calorimeter system with  $e/h = 1.6$ . This is representative for a variety of calorimeters used in particle physics experiments, and in particular for detectors based on liquid argon as active material. The third calorimeter system for which the jet responses were determined was compensating ( $e/h = 1.0$ ). A comparison of the results for the other calorimeters with the latter one would make it possible to assess the effects of non-compensation on the calorimeter response to the different fragmenting partons.

In each case, the response of a particular calorimeter to a given type of jet was determined as follows. First, the average composition of the jet was determined from the simulations. For example, we found that a  $Z^0$  produced at the Tevatron and decaying into an  $s\bar{s}$  quark-antiquark pair produced, on average, the following particles in the final state: 15.9 charged pions, 8.8  $\pi^0$ s, 3.5 kaons, and 2.2 (anti)baryons ( $p, n, \bar{p}, \bar{n}$ ). The average energies of these particles amounted to 4.4 GeV ( $\pi^\pm$ ), 4.2 GeV ( $\pi^0$ ), 13.0 GeV (K), and 8.9 GeV (baryons), respectively. In addition, small numbers of other particles were produced: 0.02  $e^\pm$  (average energy 2.4 GeV), 0.009  $\mu^\pm$  (3.4 GeV), 0.02  $\nu, \bar{\nu}$  (3.6 GeV) and 1.1  $\gamma$ s from sources other than  $\pi^0$  decay (3.3 GeV).

Next, the calorimeter response to these individual final-state components was determined, using Eqs. (1) and (2). These responses were for all calorimeters 0 for the (anti)neutrinos and 1.0 for the  $\pi^0$ s,  $e^\pm$  and  $\gamma$ s. Since we assumed that muons deposit on average 2 GeV in a typical calorimeter, the response to these particles was chosen to be  $2.0/3.4 = 0.59$ . For the other particles, the response depended on the calorimeter's  $e/h$  value. For example, the response to the charged pions (for which  $\langle f_{em} \rangle = 0.282$ ) was 1.0 when  $e/h = 1.0$ , 0.731 when  $e/h = 1.6$  and 0.641 when  $e/h = 2.0$ . The response to the kaons for these three  $e/h$  values was 1.0, 0.748 and 0.664, respectively, and the response to the (anti)baryons was 1.0, 0.735 and 0.647, respectively. The response to kaons and to (anti)baryons takes into account the fact that in the showers initiated by these particles strangeness and baryon number have to be conserved. As discussed in Section 2, this leads to a reduced response, since it precludes the production of leading  $\pi^0$ s in the shower development. Based on experimental data, such as the ones shown in Figs. 2 and 3, we decided to take

these effects into account by reducing the average em fraction ( $\langle f_{em} \rangle$ ) for these particles by 20% compared to the corresponding value for charged pions of the same energy. This would, for example, at 300 GeV lead to a proton/pion response ratio in the CMS HF calorimeter ( $e/h \approx 5$ ) of 0.85, in good agreement with the experimentally measured value (see Fig. 2).

Finally, the overall jet response was determined from the response to the individual final-state particle types, and the relative contribution of these particles to the  $Z^0$  final state. Since charged pions carried, on average, in total 39.8% of the  $Z^0$  energy in  $Z^0 \rightarrow s\bar{s}$  events, and the response to these charged pions was 0.731 in the  $e/h = 1.6$  calorimeter, these particles contributed  $0.398 \times 0.731 = 0.291$  to the s-jet response of the calorimeter. Similarly,  $\pi^0$ s contributed  $0.211 \times 1 = 0.211$ , kaons  $0.259 \times 0.748 = 0.194$  and (anti)baryons  $0.111 \times 0.735 = 0.082$ . An additional small contribution came from other  $\gamma$ s ( $0.020 \times 1.0 = 0.020$ ), while the contributions from the other mentioned particles were negligibly small. The total response of the  $e/h = 1.6$  calorimeter to  $Z^0$ s produced at the Tevatron and decaying into  $s\bar{s}$  parton pairs was thus found to be 0.798, or about 20% smaller than for the electrons with which this calorimeter was calibrated.

A similar procedure was followed to determine the jet response for all other fragmenting partons studied in this context. Results are listed in Table 1 for  $Z^0$  bosons produced at the LEP I, the Tevatron and the LHC, respectively. Also included in this Table are the responses for a subset of events in which  $Z^0$ s with energies between 800 and 1200 GeV were selected.

The table shows that the response to  $Z^0$  bosons decaying into  $c\bar{c}$  and  $b\bar{b}$  parton pairs is systematically lower than that for the other decay modes, in all calorimeters. This is a consequence of the fact that in the semileptonic decays of the c and b (anti)quarks (anti)neutrinos are produced that escape detection. Also, the muons produced in such processes typically only deposit a fraction of their energy in the calorimeter. The table also shows that the response to  $Z^0$  bosons decaying into  $s\bar{s}$  is systematically more reduced as a result of non-compensation than the response to  $Z^0$  bosons decaying into lighter parton pairs. This is a consequence of the fact that the final state of  $Z^0 \rightarrow s\bar{s}$  typically contains

**Table 1**

The calorimeter response ( $R$ , see Eq. (1)) for calorimeters with different  $e/h$  values to the decay products of  $Z^0$  bosons, produced in different processes and with different (average) energies. The calorimeter response is normalized to that for electrons. The statistical errors vary between 0.0002 and 0.0004.

Calorimeter system	$Z^0 \rightarrow u\bar{u}$	$Z^0 \rightarrow d\bar{d}$	$Z^0 \rightarrow s\bar{s}$	$Z^0 \rightarrow c\bar{c}$	$Z^0 \rightarrow b\bar{b}$
First, results for $Z^0$ s produced at rest in 91 GeV $e^+e^-$ collisions (LEP 1)					
$e/h = 1.0$	0.9997	0.9996	0.9996	0.9650	0.9160
$e/h = 1.6$	0.7913	0.7912	0.7751	0.7606	0.7246
$e/h = 2.0$	0.7218	0.7218	0.7003	0.6925	0.6608
Next, results for $Z^0$ s produced in 1.96 TeV $p\bar{p}$ collisions at the Tevatron. The average $Z^0$ energy is 176 GeV					
$e/h = 1.0$	0.9996	0.9997	0.9996	0.9631	0.9107
$e/h = 1.6$	0.8130	0.8127	0.7976	0.7795	0.7390
$e/h = 2.0$	0.7508	0.7504	0.7302	0.7182	0.6818
Next, results for $Z^0$ s produced in 8 TeV $pp$ collisions at the LHC. The average $Z^0$ energy is 415 GeV					
$e/h = 1.0$	0.9995	0.9996	0.9995	0.9620	0.9084
$e/h = 1.6$	0.8371	0.8371	0.8221	0.8018	0.7588
$e/h = 2.0$	0.7830	0.7830	0.7629	0.7485	0.7089
Finally, results for $Z^0$ s produced in 8 TeV $pp$ collisions at the LHC. Only events with $Z^0$ s carrying energies of 800–1200 GeV were selected. The average $Z^0$ energy is 975 GeV					
$e/h = 1.0$	0.9995	0.9996	0.9994	0.9608	0.9072
$e/h = 1.6$	0.8580	0.8572	0.8433	0.8207	0.7766
$e/h = 2.0$	0.8109	0.8097	0.7913	0.7739	0.7331

a considerably larger fraction of strange particles, whose response is reduced because of the limited energy fraction transferred to  $\pi^0$ s in the calorimetric absorption process.

The results listed in Table 1 are also summarized in a number of graphs. Fig. 7 shows the energy dependence of the response of a calorimeter with  $e/h = 2.0$  to  $Z^0$  bosons decaying into different parton pairs. This energy dependence is a direct consequence of the non-compensating nature of this calorimeter. In a compensating device ( $e/h = 1.0$ ), the response to  $Z^0$ s would be (almost<sup>2</sup>) independent of the production process, for all decay modes.

It is important to realize that the results shown in Table 1 and Fig. 7 do not concern individual jets, but rather combinations of all the particles observed in the various hadronic decay modes of the  $Z^0$ . Therefore, if one wants to know the energy dependence for individual jets resulting from the fragmentation of a particular parton (including gluon radiation), one has to use half the  $Z^0$  energy as the energy of this parton. In Fig. 8, the energy dependence of the response to these different types of jets is shown for calorimeters with three different  $e/h$  values. We make the following observations:

- In the non-compensating calorimeters, the response increases for all jets as a function of energy (Fig. 8b,c). This reflects the increased em component of the showering jet fragments. The energies covered by this analysis span an interval of about one order of magnitude. The increase in the jet response varies between 10.9% (b jets) and 13.0% (s jets).
- At the same energy, the response to jets resulting from fragmenting s quarks is  $\sim 3\%$  smaller than that to jets generated in the fragmentation of light quarks, for an  $e/h = 2.0$  calorimeter. This is a consequence of the fact that a larger fraction of the shower energy for such s jets is deposited by kaons, whose showers have smaller  $\langle f_{em} \rangle$  values than pions of the same energy. For example, we found that  $\sim 8\%$  of the energy contained in the  $u\bar{u}$  jets from  $Z^0$ s produced

<sup>2</sup> A very small remaining energy dependence results from the fact that muons produced in semi-leptonic decay deposit an energy dependent fraction of their energy in the calorimeter.

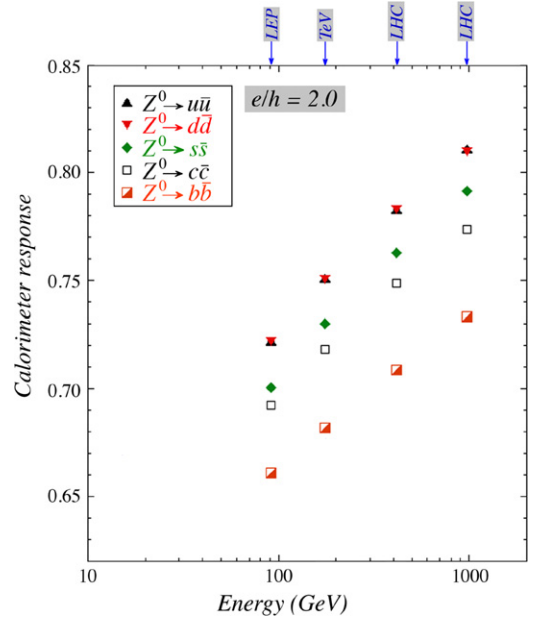


**Fig. 7.** The response ( $R$ , see Eq. (1)) of a particular calorimeter system (with  $e/h = 2$ ) to jets resulting from the fragmentation of different quark–antiquark combinations, as a function of energy. The  $q\bar{q}$  jets were the result of  $Z^0$  decay. The energy dependence was obtained by taking  $Z^0$ s produced at the Large Hadron Collider, the Tevatron or LEP. The calorimeter systems were calibrated with electrons.

at the Tevatron was deposited by kaons, versus  $\sim 34\%$  for the  $s\bar{s}$  jets.

- At the same energy, the response to c and b jets is smaller than that to jets generated in the fragmentation of light quarks by  $\sim 4\%$  and  $\sim 9\%$ , respectively (for an  $e/h = 2.0$  calorimeter). These differences are, apart from the larger kaon content that also affects the s response, mainly determined by the (anti)-neutrinos and muons produced in the semileptonic decays of these heavy quarks.
- The latter effect is also responsible for the different responses observed in *compensating calorimeters* (Fig. 8a). The response of such calorimeters is, in good approximation, independent of the jet energy.

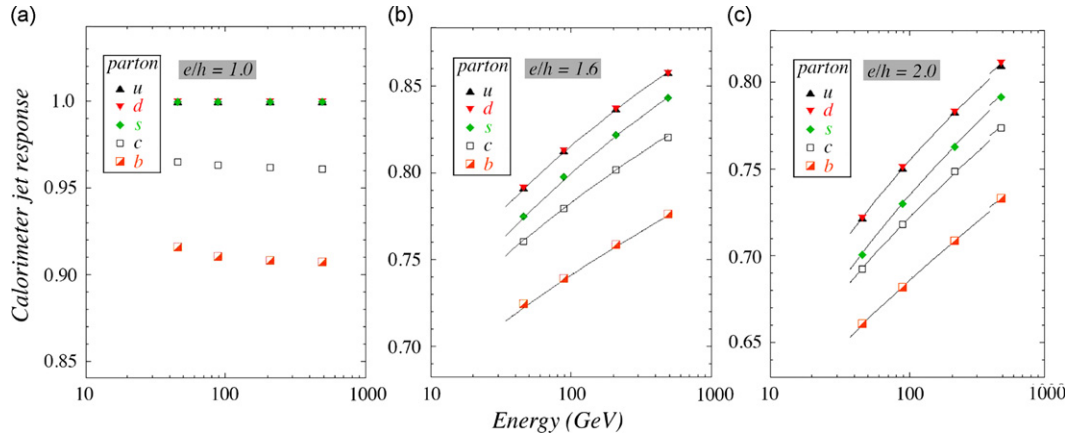


**Fig. 8.** The response ( $R$ , see Eq. (1)) of calorimeter systems with  $e/h = 1, 1.6$  and  $2$  to jets resulting from the fragmentation of individual partons, as a function of energy. The curves in diagrams b and c represent fits to a function of the type described in Eq. (3), with parameter values listed in Table 2. The calorimeters were calibrated with electrons.

**Table 2**

The values of the parameters  $p_0$  and  $p_1$  that describe the energy dependence of the jet response (Eq. (3)) for jets resulting from the fragmentation of different types of partons and for calorimeters with different degrees of non-compensation.

Parameter	u	d	s	c	b
$e/h = 1.6$					
$p_0$ (GeV)	0.0033	0.0031	0.0031	0.0004	0.00004
$p_1$	0.836	0.837	0.845	0.877	0.910
$e/h = 2.0$					
$p_0$ (GeV)	0.0168	0.0185	0.0178	0.0056	0.00115
$p_1$	0.838	0.836	0.846	0.869	0.898

The curves drawn in Fig. 8 represent an attempt to parameterize the energy dependence of the calorimeter response to the jets resulting from the fragmentation of the different types of partons. We used an expression of the same type as the one used to describe the energy dependence of the average em energy fraction in hadronic shower development (Eq. (2)):

$$R_p = 1 - \left[ \frac{E}{p_0} \right]^{(p_1 - 1)}. \quad (3)$$

The jet response data listed in Table 1 were fit to an expression of this type. The values of the coefficients  $p_0$  and  $p_1$  that gave the best fit to the data for the non-compensating calorimeters ( $e/h = 1.6, 2.0$ ) are listed in Table 2. The jet response is in practice (almost) energy independent for compensating calorimeters (see also Fig. 8a).

In Figs. 9 and 10, our simulation results are shown as a function of the calorimeter's  $e/h$  value and of the type of fragmenting parton, respectively. In both cases,  $Z^0$ s produced at Fermilab's Tevatron were chosen for this purpose. The jets from the decay of such  $Z^0$ s had an average energy of  $\sim 100$  GeV. In Figs. 9 and 10a, the calorimeter response was normalized to that for electrons. Fig. 10b shows the relative calorimeter responses to the different types of jets in a scenario in which jets from the process  $Z^0 \rightarrow u\bar{u}$  are used for the calorimeter calibration. Note the different vertical scales in these figures. Both calibration scenarios exhibit similar features. The response to fragmenting u and d quarks is about the same and larger than that to other types of quarks, except for s quarks in compensating calorimeters, for which the response is the same as for the light quarks. In non-compensating calorimeters, the response to s quarks is smaller by about 3%. The response to c and b quarks are smaller

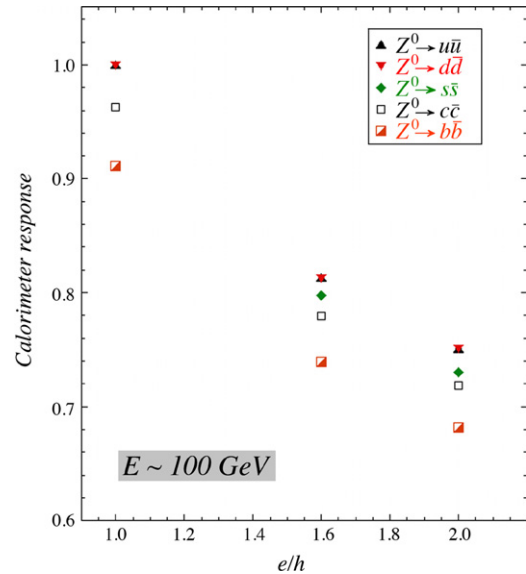


**Fig. 9.** The calorimeter response ( $R$ , see Eq. (1)) to jets resulting from the fragmentation of different partons, as a function of the degree of non-compensation (i.e., the  $e/h$  value) of the calorimeter. The (anti)quark jets were produced in  $Z^0$  decay at Fermilab's Tevatron, and had an average energy of  $\sim 100$  GeV. The calorimeter response is normalized to that for electrons.

than that to the light quarks by  $\sim 4\%$  and  $\sim 9\%$ , respectively, in all calorimeters.

The effects of the  $e/h$  value on the response are large when electrons are being used to calibrate the calorimeters. When quark jets are used for that purpose (which would be much less easy to implement in practice), the differences introduced by the  $e/h$  value are small, at maximum 3% in the case of s quarks. This feature is due to the fact that in this calibration scenario the effects of neutrinos and muons, which are primarily responsible for the reduction of the response to c and b quarks, are independent of the calorimeter's  $e/h$  value. On the other hand, these effects are somewhat dependent on the jet energy, since lower-energy muons deposit a larger fraction of their energy in the calorimeter.

#### 4.2. Multiplicity dependence

In practice, it is often not possible to recognize the type of parton that produced the jet detected in an experiment. A secondary

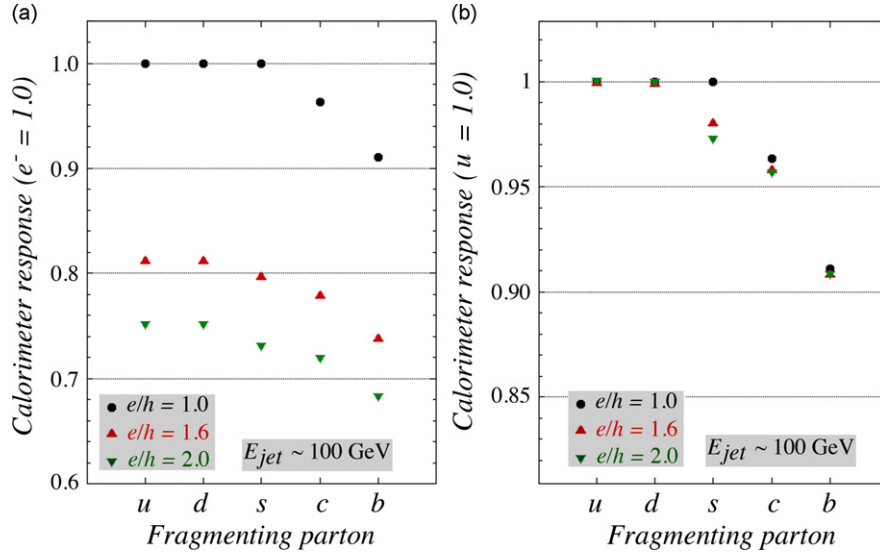


**Fig. 10.** The response ( $R$ , see Eq. (1)) of three calorimeter systems to jets resulting from the fragmentation of different types of (anti)quarks, produced in  $Z^0$  decay at Fermilab's Tevatron. The calorimeters differ in their degree of non-compensation (i.e., their  $e/h$  value). In diagram *a*, the calorimeters were all assumed to be calibrated with electrons, i.e., their response to electrons is 1.0. In diagram *b*, the calorimeters were all assumed to be calibrated with jets resulting from the process  $Z^0 \rightarrow u\bar{u}$ , i.e., their response to such  $Z^0$ s is 1.0. All jets had energies of  $\sim 100$  GeV.

vertex close to the production point is usually a telltale sign of a decaying particle containing a heavy quark, but apart from that there are very few clues in this respect. However, there are experimental features that may be used to apply the type of corrections needed to account for the effects of the non-compensation of the calorimeter system.

One jet feature that can be easily established in practice is the *charged-particle multiplicity*. In this subsection, we investigate how the calorimeter response varies as a function of this parameter, for jets resulting from the fragmentation of different partons and with energies in a given bracket. For this purpose, we selected  $Z^0$  bosons with an energy between 300 and 400 GeV, produced in 8 TeV pp collisions at the LHC. The events were grouped into sub-samples according to the charged-particle multiplicity,  $n^\pm$ , in the final state. On average, 19.4 charged particles (predominantly  $\pi^\pm$ ,  $K^\pm$  and  $p, \bar{p}$ ) were produced in these events, and the average energy of the  $Z^0$ s was 346 GeV. The charged-particle multiplicity distribution for these jets is shown in Fig. 11.

In Table 3, the response of calorimeters with  $e/h$  values of 1.6 and 2.0 to events of the types  $Z^0 \rightarrow u\bar{u}$  or  $Z^0 \rightarrow d\bar{d}$  is listed for different values of  $\langle n^\pm \rangle$ . This table also lists the multiplicity dependence of  $Z^0 \rightarrow u\bar{u}$  or  $Z^0 \rightarrow d\bar{d}$  events produced in  $e^+e^-$  collisions at 91 GeV (LEP I).

In Fig. 12, the response of a calorimeter with  $e/h = 2.0$  to  $u$  or  $d$  jets from these  $Z^0$  decays is shown as a function of the charged-particle multiplicity. For a jet of a given energy, an increased particle multiplicity means a lower average energy per jet fragment, which implies a smaller average em shower fraction and thus a smaller calorimeter response. The figure shows that these effects may be quite substantial, differences of up to 20% are observed for the LEP jets. These data show that the charged-particle multiplicity, combined with an estimate of the jet energy, provides indeed a good indicator of the effects of non-compensation on the calorimeter response. More importantly, this information could be used in practice to correct for these effects.

To avoid misunderstanding, we want to emphasize that this use of the tracker information has nothing to do with the “Particle Flow Algorithms” mentioned in Section 1. We are not substituting calorimeter information by momenta measured with the tracking system. We use the charged-particle multiplicity (*not* the momenta) to determine the effects of non-compensation on the calorimeter

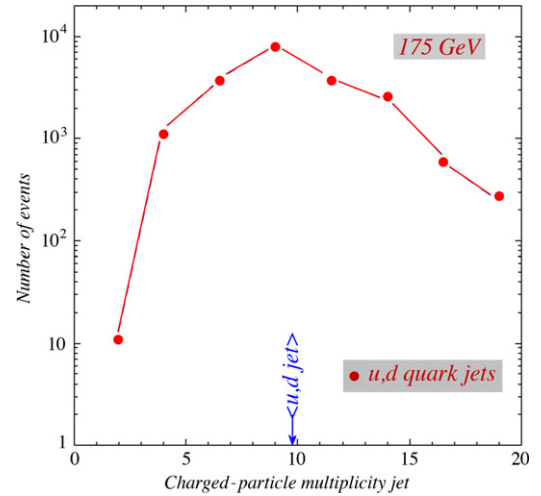


**Fig. 11.** Distributions of the charged-particle multiplicity for jets resulting from the fragmentation of light quarks, produced in  $Z^0$  decay at the LHC. The average energy of the jets is 175 GeV.

**Table 3**

The response ( $R$ , see Eq. (1)) of calorimeters with  $e/h = 1.6$  or  $2.0$  to events of the type  $Z^0 \rightarrow u\bar{u}$  or  $Z^0 \rightarrow d\bar{d}$ , for event samples with different final-state charged-particle multiplicities,  $\langle n^\pm \rangle$ . Statistical uncertainties in the last digit(s) are given in parentheses. The  $Z^0$  bosons were either produced at rest in 91 GeV  $e^+e^-$  collisions (LEP I), or in 8 TeV pp collisions at the LHC, with an energy between 300 and 400 GeV.

$\langle n^\pm \rangle$	$\langle E_Z \rangle = 91 \text{ GeV}$		$\langle E_Z \rangle = 346 \text{ GeV}$	
	$e/h = 1.6$	$e/h = 2.0$	$e/h = 1.6$	$e/h = 2.0$
4	0.857 (10)	0.809 (9)	0.891(31)	0.855 (30)
8	0.825 (1)	0.767 (1)	0.858 (3)	0.810 (3)
13	0.809 (1)	0.745 (1)	0.846 (2)	0.795 (2)
18	0.794 (1)	0.725 (1)	0.834 (1)	0.779 (1)
23	0.782 (1)	0.710 (1)	0.824 (2)	0.766 (2)
28	0.773 (1)	0.698 (1)	0.820 (2)	0.760 (2)
33	0.765 (1)	0.687 (1)	0.813 (4)	0.751 (4)
38	0.759 (2)	0.679 (2)	0.806 (6)	0.741 (6)



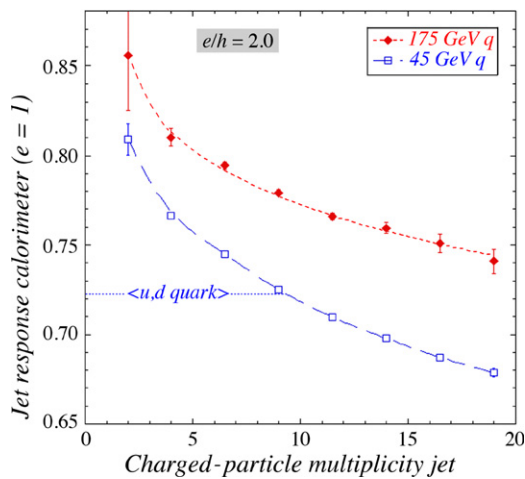


**Fig. 12.** The response of a calorimeter with  $e/h=2.0$  to jets resulting from the fragmentation of u and d quarks from the decay of  $Z^0$  bosons, as a function of the charged-particle multiplicity of these jets. The lines are drawn to guide the eye. The  $Z^0$  bosons were either produced at rest (45 GeV jets) in  $e^+e^-$  collisions at LEP I, or in 8 TeV pp collisions at the LHC (175 GeV jets). The calorimeter response is normalized to that for electrons.

response. However, the calorimeter response itself is entirely and exclusively composed of calorimeter signals.

## 5. Conclusions

We have investigated the effects of non-compensation on the calorimeter response to jets resulting from the fragmentation of different types of partons. In an era where detection of hadronic objects with a precision at the level of a few percent becomes increasingly important, and in some cases crucial,<sup>3</sup> these effects are by no means negligible. The effects can be subdivided into two classes:

- (1) The fact that some types of jets contain final-state fragments that do either not contribute at all, or at best very inefficiently, to the calorimeter signals reduces the response. This is especially true for jets resulting from the fragmentation of c and b quarks.
- (2) Since the response of non-compensating calorimeters to kaons and baryons is smaller than to charged pions of the same energy, the jet response depends on the relative contribution of such particles to the final-state composition.

In our analysis, we have only considered the fact that the average em fraction in showers induced by kaons and baryons is smaller because of the requirements of strangeness and baryon number conservation. Other effects, such as kaon decay in flight upstream of the calorimeter may also affect its response. The importance of such effects depends on the geometry of the experimental setup and the kaon energy. However, experimental data such as those shown in Fig. 3 indicate that the net result of all mentioned effects is a response reduction, at the level of the one we have taken into account in our analysis.

We have shown that in practice the effects of calorimeter non-compensation may be implemented using the measured charged particle multiplicity of the jet, in combination with an estimate of

the jet energy. This method may also be very useful for gluon jets. It is well known that the average multiplicity of gluon jets is larger than that of fragmenting quarks of the same energy [19]. Therefore, the response of a given calorimeter to gluon jets will typically be smaller than to u,d quark jets of the same energy. However, by applying corrections based on the observed charged particle multiplicity, the non-compensation effects may be properly implemented on an event-by-event basis. The jet response of compensating calorimeters is, in first approximation,<sup>4</sup> not affected by differences in charged-particle multiplicity.

The factors that reduce the response to jets resulting from the fragmentation of s, c or b quarks can only be implemented if there is evidence for the nature of the fragmenting quark, e.g., in the form of a secondary vertex, the occurrence of leptons and/or an excess of strange particles ( $K^0, \Lambda^0$ ) in the final state.

This analysis shows that, especially for non-compensating calorimeters, the tracking system may provide important additional information for increasing the precision of jet energy measurements. Yet, both the type of information and the way it is used are completely different than in PFA techniques.

## Acknowledgments

This work was supported by Grants from the US Department of Energy, under numbers DE-FG02-12ER41783 and DE-FG02-12ER41840. We thank Drs. Stephen Mrenna and Igor Volobouev for helpful discussions.

## References

- [1] D.J. Simon, in: C. Petit-Jean-Genaz, et al. (Eds.), Proceedings of the Fifth European Particle Accelerator Conference, Barcelona, Institute of Physics, Bristol, 1996, p. 295.
- [2] R.A. Beth, et al., *Science* 128 (1958) 1393.
- [3] L. Evans, P. Bryant, *Journal of Instrumentation* 3 (2008) S08001.
- [4] R. Hettel, et al., SPEAR 3 Design Report, SLAC-R-609, 1999.
- [5] G.A. Voss, *IEEE Transactions on Nuclear Science NS-26* (1979) 2970; J. Rossbach, *IEEE Transactions on Nuclear Science NS-28* (1981) 2025.
- [6] R. Wigmans, *Calorimetry—Energy Measurement in Particle Physics*, International Series of Monographs on Physics, vol. 107, Oxford University Press, 2000.
- [7] O. Lobbán, A. Sriharan, R. Wigmans, *Nuclear Instruments and Methods in Physics Research Section A* 495 (2002) 107.
- [8] D. Buskulic, et al., *Nuclear Instruments and Methods in Physics Research Section A* 360 (1995) 481.
- [9] A. Abulencia, et al., CDF Collaboration, *Physical Review D* 75 (2007) 092004.
- [10] CMS Collaboration, Particle flow event reconstruction in CMS and performance for Jets, Taus, and  $E_T^{miss}$ , CMS physics analysis summary, CMS-PAS-PFT-09-001, 2009.
- [11] Torbjörn Sjöstrand, et al., *Computer Physics Communications* 178 (2008) 852.
- [12] Fermi National Accelerator Laboratory, Design Report Tevatron 1 Project, FERMILAB-DESIGN-1984-01, 1984; L.M. Lederman, *Scientific American* 264 (1991) 26.
- [13] D. Brandt, et al., *Reports on Progress in Physics* 63 (2000) 939.
- [14] D. Acosta, et al., *Nuclear Instruments and Methods in Physics Research Section A* 316 (1992) 184.
- [15] N. Akchurin, et al., *Nuclear Instruments and Methods in Physics Research Section A* 399 (1997) 202.
- [16] T.A. Gabriel, et al., *Nuclear Instruments and Methods in Physics Research Section A* 338 (1994) 336.
- [17] N. Akchurin, et al., *Nuclear Instruments and Methods in Physics Research Section A* 408 (1998) 380.
- [18] N. Akchurin, et al., The Response of the CMS Combined Calorimeters to Single Hadrons, Electrons and Muons, CERN, Genève, Switzerland, 2007 (CMS note 2007/012).
- [19] D. Buskulic, et al., *Physics Letters B* 384 (1996) 353.
- [20] A. Andresen, et al., *Nuclear Instruments and Methods in Physics Research Section A* 290 (1990) 95.

<sup>3</sup> The ability to separate hadronically decaying W and Z bosons is considered the main design criterion for detectors at a future Linear  $e^+e^-$  collider.

<sup>4</sup> Very soft jet fragments may lose all their energy by ionization rather than through shower development. The calorimeter response to such fragments may be anomalously large [20].